Proteomic Consequences of a Human Mitochondrial tRNA Mutation beyond the Frame of Mitochondrial Translation

Petra Tryoen-Toth, Sophie Richert, Bénédicte Sohm, Manuele Miné, Cécile Marsac, Alain van Dorsselaer, Emmanuelle Leize, Catherine Florentz

THE JOURNAL OF BIOLOGICAL CHEMISTRY
Vol. 278, No. 27, Issue of July 4, pp. 24314–24323, 2003
Printed in U.S.A.

Proteomic Consequences of a Human Mitochondrial tRNA Mutation beyond the Frame of Mitochondrial Translation*

Received for publication, February 12, 2003, and in revised form, April 16, 2003
Published, JBC Papers in Press, April 24, 2003, DOI 10.1074/jbc.M301530200

Petra Tryoen-Tóth‡, Sophie Richert§, Bénédicte Sohm‡, Manuele Mine¶, Cécile Marsac¶, Alain Van Dorsselaer§, Emmanuelle Leize§, and Catherine Florentz‡‖

From the ‡UPR 9002, Institut de Biologie Moléculaire et Cellulaire du CNRS, 15 Rue René Descartes 67084 Strasbourg Cedex, §Laboratoire de Spectrométrie de Masse Bio-Organique, Ecole de Chimie des Polymères, 25 Rue Becquerel, 67087 Strasbourg Cedex 2, and ¶Laboratoire CERTO, Faculté Necker, 156 Rue de Vaugirard, 75015 Paris, France

Numerous severe neurodegenerative and neuromuscular disorders, characterized biochemically by strong perturbations in energy metabolism, are correlated with single point mutations in mitochondrial genes coding for transfer RNAs. Initial comparative proteomics performed on wild-type and Myoclonic Epilepsy and Ragged Red Fibers (MERRF) mitochondria from sibling human cybrid cell lines revealed the potential of this approach. Here a quantitative analysis of several hundred silver-stained spots separated by two-dimensional gel electrophoresis was performed in the specific case of a couple of mitochondria, containing or not mutation A8344G in the gene for mitochondrial $tRNA^{Lys}$, correlated with MERRF syndrome. Computer-assisted analysis allowed us to detect 38 spots with significant quantitative variations, of which 20 could be assigned by mass spectrometry. These include nuclear encoded proteins located in mitochondria such as respiratory chain subunits, metabolic enzymes, a protein of the mitochondrial translation machinery, and cytosolic contaminants. Furthermore, Western blotting combined with mass spectrometry revealed the occurrence of numerous isoforms of pyruvate dehydrogenase subunits, with subtle changes in post-translational modifications. This comparative proteomic approach gives the first insight for nuclear encoded proteins that undergo the largest quantitative changes, and pinpoints new potential molecular partners involved in the cascade of events that connect genotype to phenotype.

Mitochondria are the center of numerous metabolic functions of primary importance to the cell. They are responsible for the major ATP synthesis pathway and thus deliver energy through the activity of respiratory chain complexes and ATP synthase, all located in the inner mitochondrial (mt)[1] membrane. Mitochondria also contain major catabolic pathways including the citric acid cycle, fatty acid oxidation, part of the urea cycle, and a number of biosynthetic pathways such as those for heme, ubiquinol, and cardiolipin (1). To fulfill these functions, mitochondria produce a subset of 13 proteins by translation of their own genes and import a large number of proteins encoded by the nuclear genome (estimated 400–2000), translated within the cytosol. Among these are numerous proteins allowing maintenance and expression of the mt genome (replicase, transcription factors, and translation proteins). Thus, mt functions depend on well coordinated cross-talks between mt and nuclear genomes, allowing for a controlled balance between mitochondria encoded and nuclear encoded proteins and associated enzymatic activities.

Mt genomes are very sensitive to mutations (2–4). In the case of human, as many as 150 point mutations have been correlated already with various neuromuscular and neurodegenerative disorders (5–8). tRNA genes, which correspond only to about 10% of the mt genome, are particularly sensitive because they host about 80 of the known pathogenesis-associated mutations. Genotype/phenotype relationships for these disorders are complex because one mutation can be related to several disorders, and conversely a same disorder can arise from several different mutations. Due to the central role of tRNAs in protein synthesis (9), defects in structure/function relationships of mutant tRNAs have been sought (*e.g.* reviewed in Refs. 5, 6, 8, 10–13). The rate of synthesis of the 13 mitochondria-encoded proteins is decreased, and tRNA maturation, stability, post-transcriptional modification, structure, aminoacylation, and/or codon reading properties can be affected. However, depending on the specific case studied, distinct results were observed, confirming a complex relationship between genotypes and phenotypes and suggesting the contribution of additional factors to the expression of the disease (14). Furthermore, in some instances no defect in protein synthesis was observed, a discovery in support of mediators outside mt translation (15).

Comparative proteomics is a powerful approach to investigate quantitative variations in several hundred proteins at once (16, 17). Its application to human mitochondria would enlarge insight into unexpected consequences of a single point mutation in a tRNA gene on the global mt protein content. Such an approach particularly enables the analysis of the fate of nuclear encoded proteins located in mitochondria. Investigation of human mt tRNA gene mutations suffers so far from the absence of animal model systems (*e.g.* Refs. 18–20). An initial proteomic study performed on mitochondria from sibling cybrid cell lines, in the presence or absence of a single point mutation in one mt tRNA gene, has already proven the feasibility and the potential impact of such an approach for the investigation of mt

* This work was supported by CNRS, Université Louis Pasteur Strasbourg, European Community Grant QLG-CT-1999-00660, Program Physique-Chimie du Vivant from CNRS, and by the Association Française pour les Myopathies. The costs of publication of this article were defrayed in part by the payment of page charges. This article must therefore be hereby marked "*advertisement*" in accordance with 18 U.S.C. Section 1734 solely to indicate this fact.

‖ To whom correspondence should be addressed. Tel.: 33-3-88-41-70-59; Fax: 33-3-88-60-22-18; E-mail: C.Florentz@ibmc.u-strasbg.fr.

[1] The abbreviations used are: mt, mitochondrial; MERRF, Myoclonic Epilepsy and Ragged Red Fibers; MALDI-TOF, matrix-assisted laser desorption ionization time-of-flight; MS, mass spectrometry; PDH, pyruvate dehydrogenase; DTT, dithiothreitol; CHAPS, 3-[(3-cholamidopropyl)dimethylammonio]-1-propanesulfonic acid; COX, cytochrome *c* oxidase.

tRNA disorders (21). In mitochondria carrying $tRNA^{Lys}$ gene mutation A8344G, associated with Myoclonic Epilepsy and Ragged Red Fibers (MERRF syndrome (22)), a large decrease in the steady-state levels of two nuclear encoded subunits of cytochrome *c* oxidase, a respiratory chain complex, was identified upon simple visual comparison of two-dimensional PAGE (isoelectrofocusing/SDS-PAGE) followed by mass spectrometric assignment. Here the cybrid model system was further explored by a detailed computer-assisted quantitative comparison of over 800 spots obtained from wild-type and mutation A8344G-carrying mitochondria. This first large scale quantitative analysis of the protein profile of mitochondria representative of a tRNA disorder, using cybrid cell lines as a model system, revealed that in addition to the 13 mitochondria encoded proteins, all known to be affected, several nuclear encoded proteins of mt location undergo quantitative and/or qualitative changes.

The proteomic approach enlarges the view of the status of a disease-carrying cell, highlighting new molecular species relevant to perturbations within the whole cell, beyond the consequences of the primary molecular impact of a mutation on the tRNA structure/function relationship in translation. Understanding how each of these species affects the cell will shed new light on the genotype/phenotype relationships of mt disorders. Although some of the affected proteins may contribute to the expression of the disease, others may be compensating.

EXPERIMENTAL PROCEDURES

Cell Cultures

Human osteosarcoma-derived cybrid cell lines R2-1A and R1C3 were a kind gift of A. Chomyn and G. Attardi (California Institute of Technology, Pasadena). Cell line R2-1A carried the wild-type mt $tRNA^{Lys}$ gene in homoplasmic form, and cell line R1C3, associated with MERRF disease, carries an A to G transition at position 8344 in this gene in homoplasmic form (23). Cell lines were grown in Dulbecco's modified Eagle's medium with 10% fetal calf serum, 100 units/ml penicillin, 100 μg/ml streptomycin, and 100 μg/ml bromodeoxyuridine at 37 °C in the presence of 5% CO_2 and 85% humidity. R2-1A cells were seeded at a density of 2×10^5 cells/10 ml of medium/10-cm diameter Petri dish, and R1C3 cells were seeded at a density of 5×10^5 cells/10 ml/10 cm diameter. Upon reaching confluence, cells were passed (not more than 4 or 5 times), and 50–100 dishes, containing $\sim 4 \times 10^6$ cells each (confluent culture), were harvested for mitochondria isolation. Stability of the cell lines was verified in regard to the $tRNA^{Lys}$ and $tRNA^{Leu(UUR)}$ gene sequences, which were found to be unchanged over the period of experimentation.

Isolation of Mitochondria

Mitochondria were purified according to established procedures (21) with slight modifications. Briefly, cybrid cells were detached by trypsinization, centrifuged, and washed twice with cell dissociation buffer (25 mM Tris-HCl, pH 7.4, 135 mM NaCl, 5 mM KCl, 0.5 mM NaH_2PO_4). Cell pellets were resuspended in 210 mM mannitol, 70 mM sucrose, 5 mM Hepes, pH 7.2, and 2 mM EDTA (isolation buffer). Cytosolic membranes were permeabilized by a short digitonin treatment (1 min on ice, 0.04 to 0.1 mg/100 mg of total protein as measured by the Bradford technique). Permeabilization efficiency was monitored under the microscope by trypan blue staining. Cells were centrifuged, suspended in the same buffer without digitonin, and broken in a Potter-Elvehjem homogenizer with a rotating pestle up to ~80% cell breakage. The homogenate was centrifuged at $900 \times g$ for 5 min at 4 °C to remove nuclei and large debris. The supernatants were recovered and centrifuged again at $900 \times g$ for 5 min at 4 °C. This centrifugation step was repeated until the pellet became invisible (about 7–8 times). The final supernatant was centrifuged for 20 min at $10{,}000 \times g$ to collect mitochondria. Mitochondrial pellets were washed once, then resuspended in a small volume of isolation buffer, and stored at −80 °C. Protein content was estimated by the Bradford method used directly with mitochondria. Mitochondria per cell, estimated by citrate synthase activity (units per mg of total cellular protein content), was found to be similar in both cell lines (~125 milliunits/mg).

Two-dimensional PAGE

For analytical gels, samples consisted of 50–150 μg of mt protein in 100 μl of isolation buffer. For preparative gels, samples consisted of 500 μg of protein. Mitochondria were solubilized by addition of 400 μl of "lysis buffer" containing 9 M urea, 2.5 M thiourea, 5% CHAPS, 12.5 mM dithiothreitol (DTT), and 0.5% carrier ampholytes (pH 3–10) to the 100-μl mt suspension. The mixture was sonicated for 3 min before application to the strip.

Samples were deposited on linearly immobilized 17 cm long, pH 5–8 IPG strips (Bio-Rad), followed by passive overnight rehydration at 22 °C. Strips were prevented from dehydration and oxidation by covering with mineral oil (Bio-Rad). Isoelectrofocusing was performed for a total of 53,600 V-h at 22 °C (Bio-Rad, Protean IEF Cell) by application of 300 V for 2 h (to remove salt), 1500 V for 2 h (fast increasing slope), 3000 V for 16 h (focusing), and 500 V for 4 h (stabilization). Strips were equilibrated 2 times for 15 min in 0.125 M Tris-HCl, pH 7.7, 6 M urea, 30% glycerol, and 2.5% SDS, first with 65 mM DTT (reduction step), and finally with 216 mM iodoacetamide (alkylation step).

The second dimension was run after fixing each strip with 1% low melting point bromphenol blue containing agarose solution, on top of a 20 × 20-cm 10% acrylamide gel, cast in 0.2 M Tris-HCl, pH 8.1. Protein samples were electrophoresed using Tris taurine (0.05 M Tris, 0.2 M taurine, 0.1% SDS) as upper buffer (cathode), and Tris glycine (0.05 M Tris, 0.4 M glycine, 0.1% SDS) as lower buffer (anode) (21). Samples were electrophoresed at 40 mA/gel until the bromphenol blue reached the bottom of the gel (about 5 h). This allowed resolution of low molecular mass proteins down to 7 kDa. Proteins from wild-type and MERRF mitochondria were always run together in the same electrophoresis tank.

Protein Staining

Silver Staining—Gels loaded with 100–150 μg of proteins were stained according to Ref. 21. Gels were fixed overnight with 5% acetic acid, 30% ethanol, sensitized with 0.02% sodium thiosulfate for 1 min, stained with 0.2% $AgNO_3$ in ultrapure water for 90 min, developed in 4% potassium carbonate, 0.25 ml/liter formaldehyde, 0.025% sodium thiosulfate. Staining reaction was stopped by 4% Tris base (*m/v*), 2% acetic acid treatment. Gels were rinsed, scanned (GS-710 Calibrated Imaging Densitometer, Bio-Rad), and dried. This staining method is sensitive enough to detect about 800 spots on gels loaded with 100 μg of protein. For gels loaded with 50–70 μg of proteins, a more sensitive silver staining method (PlusOne Kit, Amersham Biosciences) was applied according to manufacturer's instructions.

Colloidal Blue (G-250) Staining—Preparative gels loaded with 500 μg of proteins were fixed 3 times for 30 min with 30% ethanol, 2% phosphoric acid. Gels were rinsed 3 times for 20 min with 2% phosphoric acid and then equilibrated with a solution containing 2% phosphoric acid, 18% ethanol, 15% ammonium sulfate for 30 min. Colloidal Blue G (Sigma) was added to the equilibration solution at a final concentration of 0.02%. Gels were stained for 24–36 h, washed with water to decrease background, and scanned. Finally spots of interest were excised with caution to avoid keratin contamination and stored at −20 °C until mass spectrometry analysis.

Gel Imaging and Spot Quantification

For quantitative analysis, gels were silver-stained. This method has a more restricted linear range compared with colloidal blue staining but requires about 10 times less protein for detection, an important factor when preparing mitochondria from adherent cell cultures. Comparison of spot intensities in two independent experiments revealed by either silver or colloidal blue staining lead to the same quantitative results except in the case of fairly dark (still not saturated) spots. In this latest case, intensity differences for a same spot in wild-type and mutant mitochondria were greater in blue gels. Thus, silver staining may tend to underestimate some of the spot intensity increases in two-dimensional maps.

Quantitative, computer-assisted gel analysis was carried out with the help of PD-QUEST software (Bio-Rad). Each scanned image was converted to gray scale pixel values by the program. All spot values were normalized according to total density in the gel image, which allows the precise comparison of gels even with different (high and low) backgrounds. Eleven gel couples (wild-type and MERRF mitochondria), run in parallel, were analyzed. After automatic detection, spots resulting from non-protein sources (*e.g.* dust, silver particles, and scratches) were filtered out. Operator intervention was required to set landmarks on each gel for accurate cross-gel image matching. This matching procedure resulted in a "master gel" containing all spot information of both

gels (spot size, density, quantity in volume (pixel = OD × spot surface), etc.). Spot volumes were compared across 11 "master" gels for each matched spot, and data were analyzed under Excel. Ratios of protein quantities (spot volumes) were established for corresponding spots (wild-type and mutation carrying sample), and mean values as well as standard errors were calculated.

Spot Analysis by Mass Spectrometry

Up-regulated spots were analyzed after excision from gels containing mutated mitochondria, and down-regulated spots were analyzed from wild-type mitochondria gels.

In-gel Digestion—Reduction was achieved by a 1-h treatment of the gel spots in 10 mM DTT at 57 °C. Alkylation reaction was performed using 25 mM iodoacetamide for 45 min at room temperature and protected from light. Tryptic digestion was performed in 12.5 ng/μl trypsin (Promega, V5111) in 25 mM NH_4HCO_3 (freshly diluted) at 35 °C overnight. Gel pieces were centrifuged, and 5 μl of 25% H_2O, 70% acetonitrile, 5% HCOOH were added to extract peptides. For MALDI-MS analysis, the supernatant volume was reduced under nitrogen flow to 4 μl; 1 μl of H_2O, 5% HCOOH were added, and 0.5 μl of the mix were used for analysis. For nano-LC-MS-MS, the supernatant solvent was completely evaporated in order to remove all acetonitrile from the sample. Then 10 μl of H_2O, 5% HCOOH were added and injected in the high pressure liquid chromatography system.

MALDI-MS—For MALDI mass spectrometry, mass measurements were carried out on a Bruker BIFLEX III™ MALDI-TOF equipped with the SCOUT™ High Resolution Optics with X-Y multisample probe and gridless reflector. Internal calibration was performed with tryptic peptides coming from autodigestion of trypsin, with monoisotopic masses at m/z = 842.51, 1045.564, and 2211.105. Monoisotopic peptide masses were assigned and used for data base searches. These files were then fed into the search engine MASCOT (Matrix Science, London, UK). The data were searched against the NCBI non-redundant protein sequence data base with trypsin plus potentially two missed cleavages. All proteins present in NCBI were taken into account without any pI and molecular weight restrictions. Some variable modifications were taken into account, like methionine oxidation, cysteine carbamidomethylation, and serine, threonine, or tyrosine phosphorylations. Detection of phosphorylated peptides resulted in matches at 80 Da higher masses/phosphate group, compared with non-phosphorylated peptides. The peptide mass error was limited to 50 ppm.

Nano-LC-MS-MS—Nanoscale capillary liquid chromatography-tandem mass spectrometric (LC-MS-MS) analysis of the digested proteins were performed using a CapLC capillary LC system (Micromass, Manchester, UK) coupled to a hybrid quadrupole orthogonal acceleration time-of-flight tandem mass spectrometer (Q-TOF II, Micromass). The LC-MS union was made with a PicoTip (New Objective, Woburn, MA) fitted on a ZSPRAY (Micromass, Manchester, UK) interface. Chromatographic separations were conducted on a reversed phase capillary column (Pepmap C18, 75 μm inner diameter, 15 cm length, LC Packings) with a 200 nl/min flow. The gradient profile used consisted of a linear gradient from 95% A (H_2O, 0.05% HCOOH) to 45% B (acetonitrile, 0.05% HCOOH) over 35 min followed by a linear gradient to 95% B for 1 min. Mass data acquisitions were piloted by MassLynx software (Micromass, Manchester, UK) using automatic switching between MS and MS-MS modes. Mass data collected during a LC-MS/MS analysis were processed and converted into a .PKL file to be submitted to the search software MASCOT (Matrix Science, London, UK). Searches were done with a tolerance on mass measurement of 0.25 Da in MS mode and 0.5 Da in MS/MS mode.

Western Blotting

Mitochondrial proteins derived from four independent preparations (10 μg) were run on one-dimensional 10% SDS-polyacrylamide gels (10 × 8 cm) and transferred to Immobilon P membrane (Millipore). After saturation with 5% milk powder in 20 mM Tris-HCl, pH 7.5, 0.5 M NaCl, reaction with specific antibodies (dilution 1:1000) was performed. The three different antibodies tested were anti-bovine pyruvate dehydrogenase E1 (gift of Dr. G. Lindsay), anti-bovine mt elongation factor (gift of Dr. L. Spremulli), and anti-human lysyl-tRNA synthetase (gift of Dr. K. Shiba). Each antibody was used at 1:1000 dilution. Secondary antibody was horseradish peroxidase coupled anti-rabbit IgG (dilution 1:5000), and reaction was revealed by the ECL method (Amersham Biosciences). After exposure, quantitative comparison of wild-type and mutant samples was performed with Quantity One software (Bio-Rad). Western blotting was also performed on two-dimensional gels loaded with 50–250 μg of mt proteins and probed with either of the three antibodies. Treatment of Immobilon membrane was as described above.

Pyruvate Dehydrogenase Activity

Total and basal activities were assayed by the release of $^{14}CO_2$ from [1-^{14}C]pyruvic acid, as described (24) with minor modifications. Cell lines were grown on a 6-ml dish until confluent. Each dish was harvested in 1 ml of lysis buffer (100 mM KH_2PO_4, pH 7.4, 2 mM EDTA, 1 mM DTT), frozen in liquid nitrogen, and stored at −80 °C. For the assay, cells were thawed and gently sonicated (4 pulses, microtip 20, 50%). Three dishes of each cell type were pooled, and the assay was performed in triplicate. Cells were preincubated for 10 min at 37 °C with 0.04 mM $MgCl_2$ and 0.04 mM $CaCl_2$ (basal activity) or with 16 mM $MgCl_2$ and 0.4 mM $CaCl_2$ (total activity). They were incubated for 15 min at 37 °C as described (24). The reaction was stopped with 0.1 ml of 50% trichloroacetic acid and left at room temperature for 90 min to allow capture of CO_2.

RESULTS

Model System—The protein content of mitochondria isolated from sibling cybrid cell lines, homoplasmic either for wild-type or for the MERRF mutation A8344G in the $tRNA^{Lys}$ gene, has been compared. The origin of both cybrid cell lines is an osteosarcoma cell line devoid of mitochondria, fused with enucleated myoblasts of a MERRF patient carrying mutation A8344G in a heteroplasmic form (25). Emerging cybrid cells were selected for the presence (R1C3 cells) or the absence (R2-1A cells) of mutation A8344G in the $tRNA^{Lys}$ gene in homoplasmic form. In consequence, these cell lines have the same nuclear background and are distinguished only by the presence or absence of mutation A8344G in their mtDNA. This model system has already been genetically and biochemically characterized and used to study MERRF mutation-related biochemical and molecular events (10, 21, 23, 26, 27). In the absence of transgenic mice and/or access to significant patient biopsy samples, cybrid cell lines represent the only valuable model system to evaluate direct or indirect effects of a human mt tRNA gene mutation at the cellular level and are thus used here for a comparative proteomic approach.

A major limitation in establishing mt proteomes resides in the difficulty of organelle purification and thus in the possible presence of lysosomal, peroxisomal, and cytosolic proteins in mt preparations. This is indeed a drawback when searching for the exact exhaustive protein content within a given organelle, a situation different from the aim of the present study. Here the comparative proteomic strategy was applied to highlight proteins undergoing quantitative changes when comparing wild-type and MERRF mitochondria. Due to the large amounts of protein required per analysis and to the low yield of mitochondria from adherent cybrid cell growth, purification of mitochondria was limited to differential centrifugations, so that contaminants on two-dimensional maps were not unexpected.

Two-dimensional PAGE of Total Mitochondrial Proteins and Quantitative Aspects—Well resolved silver-stained two-dimensional maps of mt proteins were obtained in a reproducible manner according to procedures established previously (21) and allowed detection of about 800 spots (Fig. 1). Quantification was performed on 11 gel couples to allow for a significant analysis by comparison of spot intensities, measured as spot volumes. Normalization of gels (loaded with the same amount of mt proteins), done either according to the total quantity in valid spots or to the total density in gel, leads to the same results and allowed differences linked to experimental procedures (protein loading and staining) to be eliminated so that only significant variations related to the type of sample (wild-type or mutant) were considered. For the same spot, intensity varied on average by 20–40% over the different gels of the same type (*i.e.* within all wild-type or all mutant gels). Accordingly, spot intensity variations greater than these values were

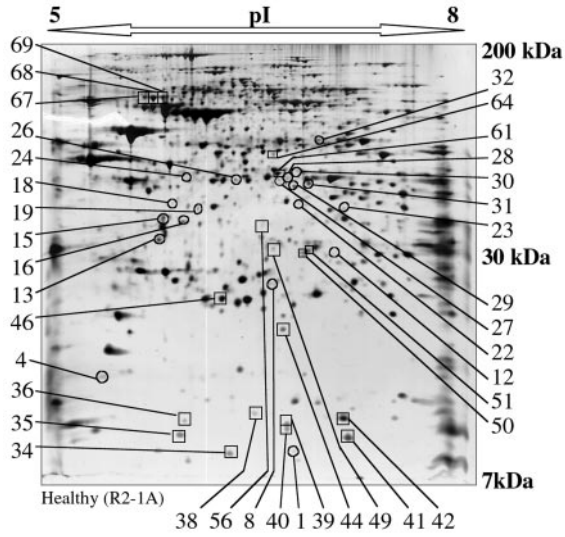

FIG. 1. **Typical silver-stained two-dimensional gel electropherogram of wild-type mitochondria from cybrid cells (R2-1A) and location of protein spots that undergo quantitative changes when compared with A8344G mutation-carrying mitochondria.** Mitochondria were purified from adherent cell lines and solubilized by high concentration of denaturing agents and non-ionic detergents to recover a large proportion of hydrophobic proteins. Proteins were separated by isoelectrofocusing (pH 5–8) followed by electrophoresis on a 10% polyacrylamide-SDS gel. Silver-stained gels were scanned and quantified using PD-Quest software. Spots that display a greater than 2-fold decrease are indicated by *open squares*, and those displaying a greater than 2-fold increase are shown by *open circles*. Spot numbers at the sides of the gel are also relevant for later figures.

sought when comparing normalized wild-type and MERRF-related two-dimensional maps. Change by a factor 2 was chosen as the basis for systematic comparison.

The majority of the spots (about 760) did not show significant intensity variations between wild-type and mutant gels. Altogether, 38 spots (4.75% of detectable spots) were found to be affected in intensity, 19 of which decreased and 19 increased. They are located all over the two-dimensional gels, covering small as well as large molecular weight domains and all the pI ranges considered (Fig. 1). Fig. 2, *A* and *B,* summarizes quantitative variations of these individual spots as an outcome of the 11 independent experiments. The range of differential spot intensities between wild-type and MERRF mitochondria varied from 2.1- to 9-fold, with most spots affected 2–5-fold. The majority of affected spots had low expression levels, with 27 spots out of 38 with intensities under 700 pixels, the highest intensity reaching 3700 pixels in both types of samples.

Spot Assignment—Differentially expressed protein spots as well as a number of non-affected spots were assigned by mass spectrometric (MS) techniques. Identification (in 2–3 independent experiments) was mainly done by MALDI-TOF on colloidal blue-stained gels, based on a minimum of 3 or 4 matching peptides with a peptide mass tolerance of 50 ppm. A typical case is shown in Fig. 3. Nano-LC-MS-MS, an approach leading to the amino acid sequence of a given peptide, was used as a complementary technique in some instances (Fig. 4). For some spots, identification was not successful (lack of signal for spots of low density, recovery of only a few peptides for proteins of low molecular weight, proteins poor in trypsin cleavage sites, low efficiency of peptide extraction from gel, etc.).

Table I lists identified spots. Most proteins correspond to nuclear encoded mt proteins, but some were cytosolic contaminants. All proteins of expected mt location appeared at gel coordinates in the range of molecular weight and pI values of their mature forms, and no peptides issued from the targeting signals were detected by MALDI analyses. Differences between theoretical and experimental pI were accounted for either by distortions in the pH gradient or by post-translational modifications of the corresponding protein (see below).

Spots with *decreased* intensities in MERRF mitochondria as compared with wild-type mitochondria were assigned principally as nuclear encoded subunits of respiratory chain complexes, especially from complex IV or cytochrome *c* oxidase (COX VIa (spot 41), COX Vb (spot 42), and COX VIb (spot 34)) and complex I or NADH ubiquinone oxidoreductase (subunits 13 (spot 35) and 24 kDa (spot 46) as well as three isoforms (same molecular weight but slightly different pI values) of the 75-kDa subunit (spots 67, 68, and 69)). Furthermore, mitochondrial ornithine aminotransferase (spot 61), a protein involved in arginine metabolism, underwent a 2.8-fold decrease in intensity, and 2 isoforms of peroxisomal enoyl-CoA hydratase (spots 50, 51) underwent a 2.1–3.1-fold decrease.

Within spots of *increased* intensity, 4 have been assigned as proteins of mt location. They correspond to subunits of the metabolic enzyme pyruvate dehydrogenase (PDH) subunit E1α (spot 28), an isoform of this protein (spot 31) and subunit E1β (spot 16). Several non-mitochondrial proteins such as cytosolic translation elongation-factor 1γ (spot 30), septin 2 (spot 27), β-actin (spots 13 and 15), guanine nucleotide-binding protein subunit β3 (spot 13), and lysosomal tripeptidyl peptidase (spot 24) were also detected.

A series of spots showing no quantitative changes have also been assigned. They include a 75-kDa heat shock protein, subunits of succinate dehydrogenase (complex II of the respiratory chain), isocitrate dehydrogenase, succinyl-CoA synthetase, pyrroline-5 carboxylate reductase, prohibitin, and metaxin 2 (results not shown).

Perturbations within Pyruvate Dehydrogenase E1—Spots of increased intensity in MERRF mitochondria are of particular interest because they reveal active molecular events taking place. This is mainly the case for PDH E1 subunits. The pyruvate dehydrogenase complex plays a central and strategic role in the control and use of carbohydrates as source of oxidative energy or as precursors of fatty acid biosynthesis (28). It is formed of three enzymes, namely pyruvate dehydrogenase (PDH E1), dihydrolipoyl *trans*-acetylase (PDH E2), and dihydrolipoyl dehydrogenase (PDH E3). PDH E1 is a heterotetramer ($\alpha_2\beta_2$).

To understand differences in gel coordinates of spots 28 (~43 kDa, pI 6.8) and 31 (~42 kDa, pI 6.9), assigned as the same protein PDH E1α, the presence for post-translational modifications was investigated with particular attention to possible phosphorylation. Indeed, negative charges of phosphates are the best candidates to influence the pI of proteins. New data bank searches performed with peptide masses, so far not included in the assignments, combined with screening for phosphorylation on serine, threonine, or tyrosines fitted with the possibility that PDH E1α extracted from spot 28 was phosphorylated at least at 4 positions (Ser-312, Ser-314, and two positions out of Ser-275, Thr-286, and Tyr-287) and that PDH E1α isoform extracted from spot 31 was phosphorylated at least at 5 different positions (Thr-35, Thr-124, Thr-126, Ser-130, and Thr-139) (Table II). However, because phosphorylation lowers the pI of a protein by about 0.2 units/phosphate group, protein in spot 28, migrating at lower pI coordinates on the two-dimensional gel than spot 31, is likely phosphorylated to a higher extent than the protein in spot 31 (see location of spots in Fig. 1 and Fig. 5*A*). The definite degree of phosphorylation of each subunit escapes MS analysis because of intrinsic limitations of this technique (incomplete extraction of hydrophobic pep-

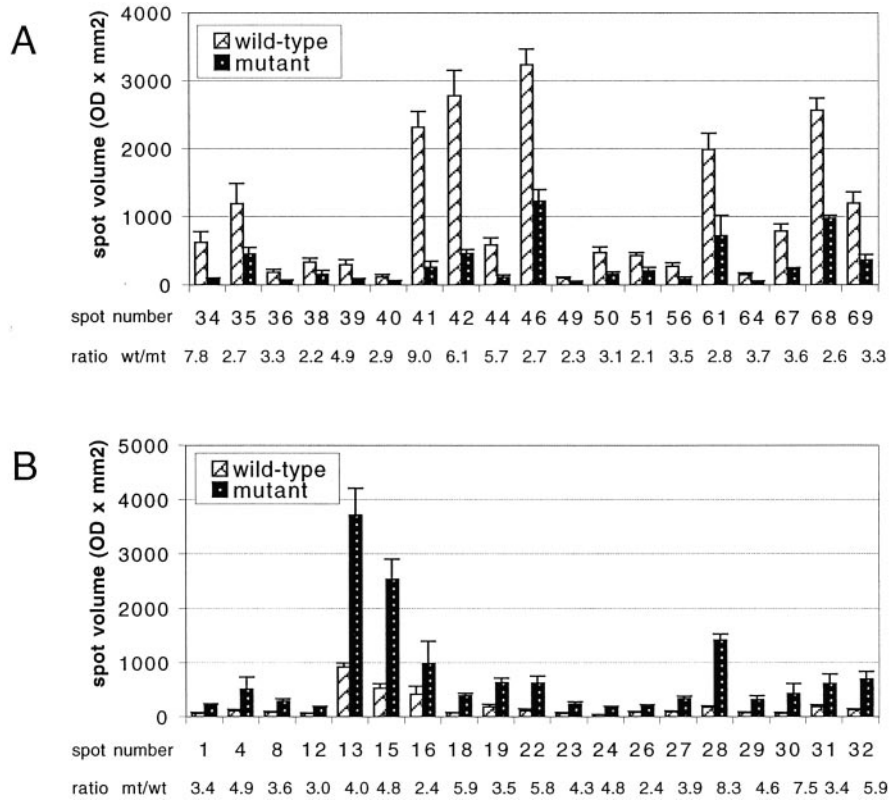

FIG. 2. **Detailed quantitative view of variations in spot intensity between wild-type and MERRF mutation-carrying mitochondria.** Only spots exhibiting greater than 2-fold changes in their quantity are reported. *A*, histogram of the 19 spots with decreased intensities in mutant mitochondria. Ratios of intensities in wild-type/MERRF mitochondria (*wt/mt*) are indicated. The range of decrease in spot intensities varies between 2.1- and 9.0-fold. *B*, histogram of the 19 spots of increased intensities in MERRF mitochondria as compared with wild-type mitochondria. Here ratios of spot intensities in mutant over wild type are given. The range of spot intensity increment varies between 2.4- and 8.3-fold. *Bars* for wild-type mitochondria are indicated in *white*, and *bars* for mutant samples are indicated in *black*. Mean values of 11 independent experiments with corresponding standard errors are given.

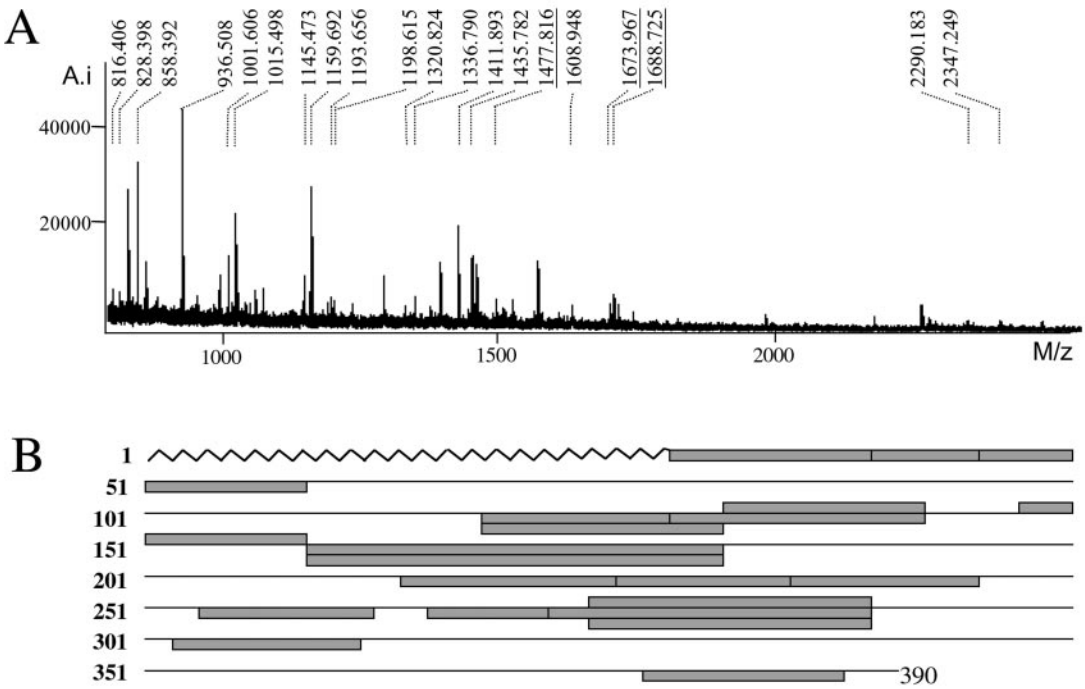

FIG. 3. **Representative result of MALDI-TOF mass spectrometric assignment.** *A*, MALDI-TOF mass spectrum of in-gel tryptic peptides, extracted from spot 31, identified as pyruvate dehydrogenase E1α subunit. Masses of the matching peptides allowing for identification are indicated, and masses of phosphopeptides are *underlined*. *B*, linear representation of the polypeptide chain with matching peptides indicated in *gray*. The protein sequence coverage was 42%. Amino acids forming the mt signal peptide are indicated at the N terminus of the sequence by a *zig-zag line*. No matching peptides were found in this domain, in support to the absence of the targeting signal of the protein analyzed.

tides from gels, non-detectable peptides) and remains so far unknown.

Although in wild-type mitochondria intensities of spot 16 (subunit β) and spots 28 + 31 (subunits α) fit with a 1 to 1 stoichiometry, this is not the case in MERRF mitochondria (Fig. 2). Thus, additional spots corresponding to alternative isoforms of PDH E1 subunits were suspected to be present in two-dimensional gels. To investigate this possibility further, two-dimensional gels with healthy and MERRF mt proteins were submitted to Western analysis in the presence of antibodies directed against the PHD E1 ($\alpha_2\beta_2$) (Fig. 5, *B* and *C*). This approach, which is much more sensitive than silver staining,

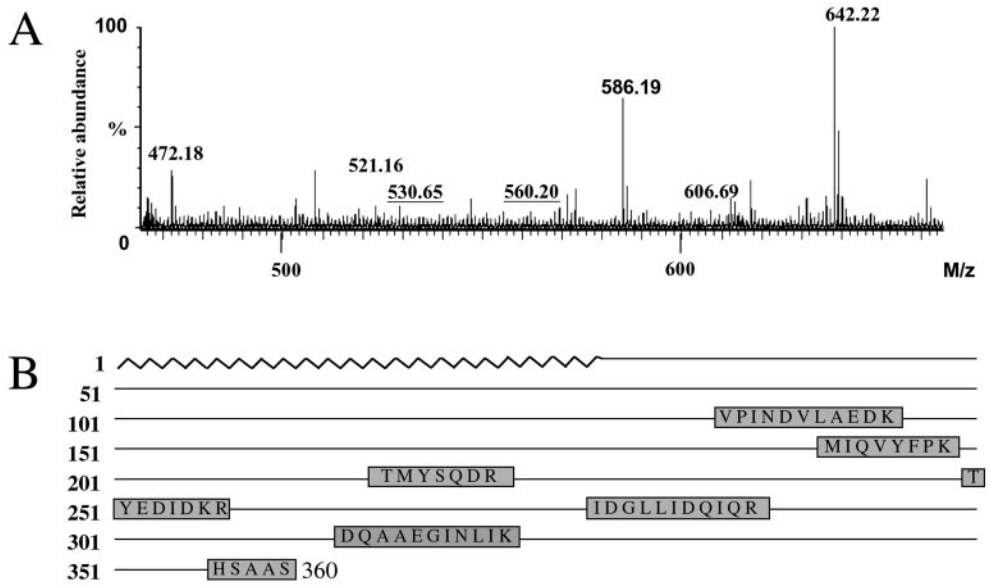

FIG. 4. **Representative result of a nano-LC-MS-MS analysis.** *A,* combined spectrum (retention time from 15 to 50 min) of in-gel tryptic digested peptides of spot 22, identified as the mt 28 S ribosomal protein MRP-S22. Masses of peptides allowing identification are indicated. *B,* linear representation of the polypeptide chain with sequences of matching peptides. Total sequence coverage was 16%. No match for the mt target signal (*zigzag line*) was found.

TABLE I

Assignment of proteins in spots undergoing quantitative changes

Spots are listed according to numbers shown in Fig. 1. Two classes of spots are distinguished: ↓, spots with decreased intensities in MERRF samples as compared with wild-type mitochondria; ↑, spots with increased intensities in mutant samples. Protein assignment was done by mass spectrometric approaches. Variations in spot intensities are expressed as ratios of either wild-type/mutant (wt/mt) or mt/wt. Names of protein, SwissProt data bank accession numbers, subcellular localization, theoretical molecular weights or isoelectric points (calculated for the mature forms of the proteins), and % of mass coverage for peptides allowing for assignment, are indicated. Loc., subcellular localization; Mt, mitochondria; C, cytosol; L, lysosome; Px, peroxisome.

Experimental			Data bank exploration					
Spot Number	Ratio	Molecular mass/pI	Protein name	Accession no.	Loc.	Molecular mass	pI	Mass coverage
↓	Decrease in intensity							
		kDa				*Da*		
35	−2.7	12/6.05	NADH/ubiquinone oxidoreductase, 3-kDa subunit	Q16718	Mt	13.327	5.77	68
46	−2.7	25/6.2	NADH/ubiquinone oxidoreductase, 24-kDa subunit	P19404	Mt	23.760	5.71	45
67	−3.6	78/5.6	NADH/ubiquinone oxidoreductase, 75-kDa subunit	P28331	Mt	77.053	5.33	37
68	−2.6	78/5.7	NADH/ubiquinone oxidoreductase, 75-kDa subunit	P28331	Mt	77.053	5.33	28
69	−3.3	78/5.8	NADH/ubiquinone oxidoreductase, 75-kDa subunit	P28331	Mt	77.053	5.33	52
42	−6.1	16/7.15	Cytochrome *c* oxidoreductase, subunit Vb	P10606	Mt	10.613	6.74	34
41	−9.0	13/7.2	Cytochrome *c* oxidoreductase, subunit VIa	Q02221	Mt	9.750	6.97	62
34	−7.8	10/6.4	Cytochrome *c* oxidoreductase, subunit VIb	P14854	Mt	10.061	6.79	65
61	−2.8	44/6.7	Ornithine aminotransferase	P04181	Mt	44.808	5.72	28
50	−3.1	33/6.8	Enoyl CoA hydratase	Q08426	Px	35.816	8.07	22
51	−2.1	34/6.9	Enoyl CoA hydratase	Q08426	Px	35.816	8.07	21
↑	Increase in intensity							
28	+8.3	43/6.8	Pyruvate dehydrogenase subunit E1α	P08559	Mt	40.229	6.51	28
31	+3.4	41/6.9	Pyruvate dehydrogenase subunit E1α	P08559	Mt	40.229	6.51	42
16	+2.4	35/6.0	Pyruvate dehydrogenase subunit E1β	P11177	Mt	35.890	5.38	31
22	+5.8	38/6.8	Mt ribosomal protein 28 S subunit S22	P82650	Mt	41.280	7.70	31
30	+7.5	47/6.8	Elongation factor-1γ	P26641	C	50.119	6.25	28
15	+4.8	38/5.85	β-Actin	P02570	C	41.053	5.56	44
13	+4.0	35/5.8	β-Actin+ guanine nucleotide-binding protein subunit β3	P02570+ P16520	C C	41.053 37.221	5.56 5.39	44 37
27	+3.9	43/6.7	Septin 2	Q15019	C	41.487	6.15	57
24	+4.8	43/6.05	Lysosomal tripeptidyl peptidase	O14773	L	39.790	5.61	35

indeed revealed the presence of additional spots aligned either with spots 28–31 or with spot 16. MALDI-TOF analysis of one spot in each of the two domains of interest in a corresponding colloidal blue-stained gel (the only spots seen on blue gels, namely spots 9 and 20), confirmed an additional subunit α (spot 20, with 39% sequence coverage) and subunit β (spot 9, with 52% sequence coverage), respectively, both with phosphorylation sites (not shown). Thus, the distribution of PDH E1 subunits into different isoforms is strongly perturbed in MERRF mitochondria.

Comparison of Western blots showed not only large qualitative but also significant quantitative differences (Fig. 5, *B* and *C*). Complementary analysis by Western blotting on a one-dimensional 10% polyacrylamide/SDS gel revealed that α and β subunits are present in equimolar amounts in both wild-type and mutated samples (not shown) and that the total quantity of

TABLE II

Phosphorylated peptides in isoforms of pyruvate dehydrogenase E1 subunits

Masses of phosphorylated peptides are shown according to experimental data by MALDI-TOF (M_r observed), to data bank derived values (M_r expected), and to "normalized" data (M_r calculated). Phosphorylation sites are underlined in peptide sequences, and the number of phosphorylations is indicated. The peptides reported here probably correspond only to a subset of phosphorylation sites. Tryptic peptides corresponding to regulatory sites already reported for the enzyme are not detected by MALDI-TOF MS, probably due to their high hydrophobicity and acidic pI.

M_r observed	M_r expected	M_r calculated	Amino acids	Peptide sequence	No. of phosphates
Spot 28 (E1α)					
1307.63	1306.62	1306.56	312-321	SKSDPIMLLK	2
1768.77	1767.76	1767.77	275-288	SGKGPILMELQTYR	2
Spot 31 (E1α)					
1477.82	1476.81	1476.66	29-40	NFANDATFEIKK	1
1673.97	1672.96	1672.79	128-141	GLSVREILAELTGR	2
1688.73	1687.72	1687.67	120-132	AHGFTFTRGLSVR	3

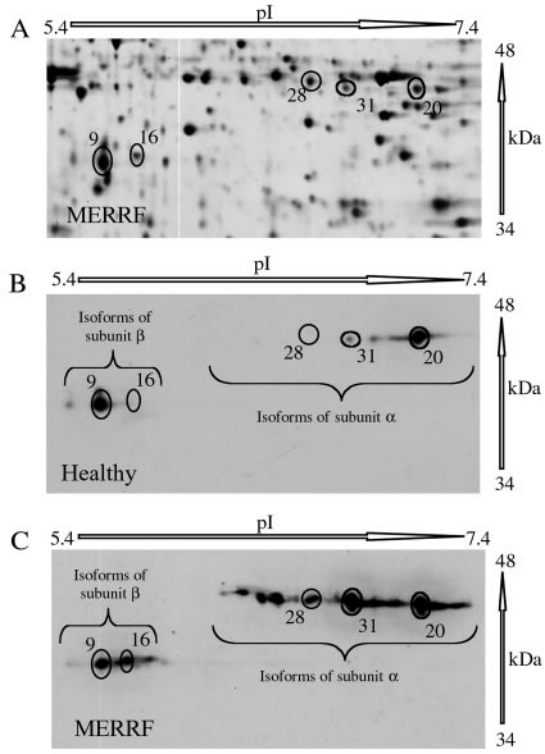

FIG. 5. **Detection of pyruvate dehydrogenase E1 subunit isoforms by Western blotting.** *A*, detail of a silver-stained two-dimensional gel of MERRF mutation-carrying mitochondria with spots assigned by MALDI-TOF as PDH E1 subunits α (spots 28 and 31) and subunit β (spot 16) indicated. *B* and *C*, Western blots of the same domain of non-stained two-dimensional gels performed with antibodies directed against PDH E1 holoenzyme. *B* corresponds to a wild-type mt sample, and *C* corresponds to a MERRF mitochondria. Immunoreactivity for β subunit resulted mainly in one major spot in wt (spot 9) and four spots in mutant samples. Immunoreactivity for α subunits resulted in a major spot (20) in wt, and to a large row of spots of the same molecular weight (about 40 kDa) in the mutant sample. Within all these newly detected spots, two were detectable on colloidal blue-stained two-dimensional gels (*9* and *20*) and have been further analyzed. MALDI-TOF measurements support the assignment of phosphorylated isoforms.

PDH E1 subunits increased about 2-fold in MERRF samples compared with wild type.

PDH E1 activity is under control of phosphorylation/dephosphorylation at well defined sites of E1α (28). Both forms (phosphorylated and non-phosphorylated) co-exist in a given cell and allow for sensitive regulation by shifting their balance. It is possible to measure basal activity, representative of the non-phosphorylated population of enzyme, and total activity subsequent to dephosphorylation by calcium and magnesium activation of phosphatases (24). Neither basal nor total activities are significantly different in wild-type and MERRF mitochondria in the presence of pyruvate as substrate (Table III).

TABLE III

Activity of pyruvate dehydrogenase in wild-type and MERRF mutation containing mitochondria (pmol/min/mg of total cellular proteins)

Each activity was measured in triplicate on cell extracts pooled from three cell cultures.

	Wild type	MERRF
Basal activity	187	141
Total activity	641	673

DISCUSSION

Comparative proteomics, combining high resolution of proteins with mass spectrometry techniques for rapid assignment, have presently been recognized as a powerful tool for the investigation of a number of human diseases (*e.g.* Refs 17, 29, and 30) including mt disorders (31–33). Further, proteomic maps of mammalian mitochondria become progressively presented in the case of human placenta (34) and rat liver (35).

Couples of cybrid cell lines form a valuable model system to investigate biochemical and molecular consequences of a mutation in the mt genome because they possess the same nuclear background and differ by a single point mutation (36). Osteosarcoma-derived cybrids were used previously to study the physiological, biochemical, and molecular effects of the A8344G mutations in the mt $tRNA^{Lys}$ gene which is correlated to the maternally inherited MERRF syndrome (22). MERRF cells have a decreased growth rate, lower oxygen consumption, and reduced cytochrome *c* oxidase activity and ATP synthesis, so that the cell undergoes a severe energy deficit (25, 27). At the molecular level, mt protein synthesis is severely impaired, and the steady-state level of the 13 mitochondria encoded proteins is decreased according to their lysine content (26). Initial comparative proteomics on these cybrid cell lines revealed that at least two nuclear encoded proteins of mt location (COX subunits Va and VIb) have severely decreased steady-state levels (21). The fate of the 13 mitochondria-encoded proteins cannot be explored by two-dimensional gel analysis due to their hydrophobicity and/or their extreme pI (34). The present work, exploring silver-stained gels on a computer-assisted basis, enlarges the knowledge of the fate of about 800 proteins contained in MERRF mitochondria compared with wild type.

Variations in Steady-state Levels of Non-mitochondrial Proteins—Assignment of regulated spots as non-mitochondrial proteins was not unexpected because mitochondria were not purified to completion. Several of these proteins are eliminated when mitochondria are further purified on a metrizamide gradient before their analysis on two-dimensional gels (results not shown). However, the very low yield of this purification procedure prevented its systematic use in the present work. The fact that certain contaminants systematically co-purify with al-

tered proportions in MERRF mt samples suggests that their detection is significant and may have a link with the pathological status of the whole cell. They may be linked to biochemical perturbations (*e.g.* acidification of the cytosol, change in ionic concentrations, and variation in mt membrane potential (37–39)) leading to alterations in physicochemical properties of these proteins. Some cytosolic proteins may become bound more or less tightly to the outer mt membrane. Alternatively, detection of quantitative changes in cytosolic proteins may reflect true molecular long range effects of the mt tRNA gene mutation such as overexpression or down-regulation of cytosolic proteins. This awaits further experimentation.

Decrease in Nuclear Encoded Subunits of Respiratory Chain Complexes—Among the 38 protein spots found to be quantitatively affected, 6 were assigned as nuclear encoded subunits of the respiratory chain complexes, *i.e.* subunits of complex I and of complex IV. Interestingly, those affected subunits from the same complex were decreased by the same factor, *i.e.* about 7.5-fold for complex IV subunits and about 3-fold for complex I subunits.

Complexes of the mt respiratory chain (with the exception of complex II) are composed of both mt and nuclear encoded subunits assembled into functional entities in the inner mt membrane. The stoichiometric assembly of these complexes necessarily depends on a well organized nucleo-mitochondrial communication allowing for fine-tuning of the expression levels of the corresponding genes in both genomes (40, 41). Although a strong decrease in steady-state levels of any nuclear encoded mt protein could result from different molecular regulatory events taking place either at the gene expression level (transcription and translation) or at the mt import level, it is likely, as suggested earlier (21), that the decreases observed here for nuclear respiratory chain subunits are the direct consequence of their degradation. Indeed, because mtDNA encoded subunits are synthesized at a lower rate, as a direct consequence of the tRNA mutation (26), their nuclear partners likely remain nonassembled and are therefore degraded. Such a situation has been demonstrated for COX nuclear encoded subunits in cell lines deprived of mtDNA or where mt translation has been inhibited (42–46). Interestingly, subunits from complex II (succinate dehydrogenase), which are all nuclear encoded and are thus not linked to mt translation, were not found to be regulated in the present work.

The five mt respiratory chain complexes are formed from 83 different subunits, of which only 13 are of mt origin. Only 6 of the 70 nuclear encoded subunits were found to be down-regulated here. The fate of the 64 remaining subunits is thus uncertain. Calculation of theoretical molecular weight and pI values for each subunit revealed that at least 22 of them should have coordinates within the two-dimensional gels studied in the present work. Their absence could reflect either their membrane location and thus difficulty to be extracted (in the x-ray structure of complex IV (47), the three subunits detected here are located on the matrix and intermembrane surfaces of the enzyme rather than within the membrane), their presence within spots which could not be assigned, or that they are not regulated or are regulated below a 2-fold factor.

Variation in Steady-state Levels of Proteins Involved in Mitochondrial Translation—Due to impairment of mt translation by mutation A8344G in the $tRNA^{Lys}$ gene, effects on proteins involved in the translational machinery may be affected. Only one ribosomal protein, MRP-S22, was found in increased quantity in MERRF mitochondria (about 6-fold). The regulation of the steady-state level of only one of the ~80 proteins which form the mt ribosome is surprising. Protein MRP-S22 belongs to a new class of ribosomal proteins, specific to mammalian ribosomes (48, 49). This protein may well have an additional alternative function, so far unknown, as observed for other newly discovered mt proteins. MRP-S29 is a death-associated protein involved in apoptosis (50), and MRP-S31 is associated with type 1 diabetes (51). To explore further possible variations in proteins belonging to the mt translational machinery, Western blotting with antibodies directed against human lysyl-tRNA synthetase (the enzyme which catalyzes aminoacylation of $tRNA^{Lys}$, the tRNA bearing the MERRF mutation investigated here) and against mt translation elongation factor Tu was performed. No significant changes in the steady-state levels of these two particular proteins were found (not shown).

Variations in Steady-state Amounts of Metabolic Enzymes—Two metabolic enzymes were found to be affected in MERRF cells. Mitochondrial ornithine aminotransferase decreased, and pyruvate dehydrogenase subunits E1α and E1β increased. Ornithine aminotransferase participates in amino acid metabolism, catalyzing inter-conversion of ornithine and glutamate. The contribution of the decrease of ornithine aminotransferase to the pathological status of the cybrid cells remains unclear. However, reduced activity of the respiratory chain correlates directly with reduced activity of the Krebs cycle, which in turn is linked via α-ketoglutarate to glutamate. Interestingly, a reduced activity of this enzyme was observed previously in the brains of Huntington's disease-affected patients. Huntington's disease is associated with the deficiency of the neurotransmitter glutamate and of mt oxidative phosphorylation (52).

The pyruvate dehydrogenase complex converts pyruvate into acetyl-CoA and has thus a central role in energy metabolism. Comparative proteomics associated with Western analysis revealed that (i) the total amount of PDH E1 subunits increased about 2-fold in MERRF mitochondria, and (ii) both subunits α and β of this enzyme are distributed over a series of isoforms in the wild-type sample, but this distribution is wider in the mutated sample. MALDI-TOF assignments are in favor of a variation in the number and distribution of phosphorylation sites as post-translational modifications in the different isoforms. The detected phosphorylation sites differ from those involved in regulation of PDH E1 activity (53) in agreement with maintenance of the same enzymatic PDH activity in both wild-type and MERRF cell lines. Whereas full understanding of biochemical and molecular perturbations of the PDH complex and their relationships with the presence of the MERRF mutation in the mt genome awaits further experiments, it is important to notice that the results of the present investigation do not preclude on the activity of the PDH complex *in vivo*. Indeed, in addition to phosphorylation/dephosphorylation at three specific sites, the activity of the complex can be allosterically regulated by NADH and acetyl-CoA (28). Both compounds accumulate in mitochondria as a consequence of respiratory deficiency. As an outcome of the present data, it is tempting to speculate that accumulation of the enzyme may represent a compensatory mechanism by the cell to overcome the energetic deficiency but that parallel activation of kinase(s) hinders effective changes in activity. Interestingly, a case of up-regulation of the amounts of PDH E1 proteins has been reported recently for butyrate-treated human colon cancer cells (54).

Expectation for Further Variations—Comparative proteomics allowed for an enlarged view of quantitative and qualitative changes in about 800 protein spots observed on two-dimensional gels from wild-type mitochondria and mitochondria containing a single point mutation in a tRNA gene. The present analysis revealed 38 affected spots, of which 20 could be assigned, and about 760 unaffected spots. As a major outcome, mitochondria with mutation A8344G in the $tRNA^{Lys}$ gene show

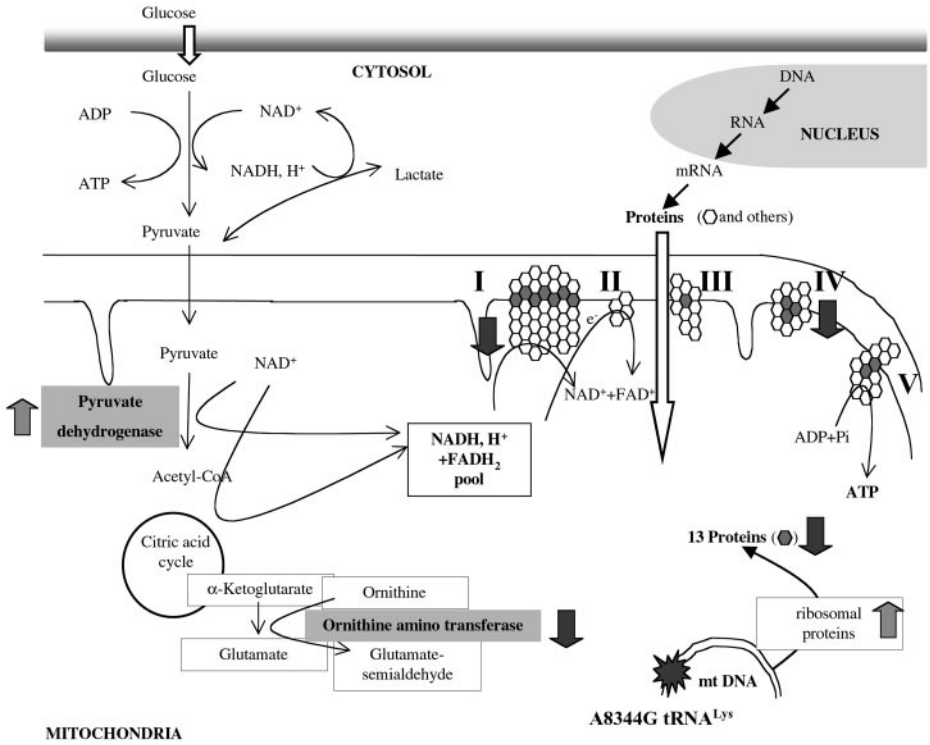

FIG. 6. **Schematic representation of the most dramatic perturbations observed by comparative proteomics on two-dimensional silver-stained gels in mitochondria harboring tRNA^{Lys} gene mutation A3243G.** Mt and nuclear gene expression machinery are considered, and their convergence at the level of respiratory chain complexes is illustrated. Major relevant energetic metabolic pathways and their connections to the respiratory chain are indicated. Decreases and increases in protein spots as seen on two-dimensional gels are indicated by *arrows*. Decreases in the 13 mt encoded subunits of the respiratory chain complexes as described (*e.g.* Ref. 26) were not observed on two-dimensional gels due to their hydrophobicity.

significant perturbations in the steady-state amounts of proteins involved in translation (MRP-S22), respiration (respiratory chain subunits), and carbohydrate and amino acid metabolism (PDH, ornithine aminotransferase). Also a series of proteins of cytosolic location were reproducibly found to be affected (either increased or decreased). These results demonstrate that the presence of a single point mutation in an mt tRNA gene not only affects mt translation but also several categories of nuclear encoded proteins, both of mt and cytosolic location. Possible links between these proteins and the mutation in an mt tRNA gene are schematized in Fig. 6.

However, it must also be stated that the number of changes observed in the MERRF cell line is rather limited in regard of the severity of the physiological and energetic perturbations taking place. The observed quantitative variations reveal only the strongest intensity changes taking place (variations of 2.1–9-fold) and certainly correspond only to a subset of molecules that undergo perturbations in the disease-related cells. Sensitive quantitative variations within a 2-fold range may be significant biologically and relevant. They escape the present analysis, however, due to limited accuracy and reproducibility. As discussed above, the fate of many respiratory chain complex subunits escaped analysis. Furthermore, changes in enzymes involved in the glycolytic pathway or those involved in other energy-related pathways would be expected to be affected. Thus, it is likely that only the "tip of the iceberg," in regard to regulatory events taking place in mitochondria, was detected so far. Many proteins may well have escaped the present analysis due to technical limitations including limited sensitivity of silver-stained gels for poorly represented proteins, analysis of basic and hydrophobic proteins, and difficulty in assignment of some proteins (especially those of low molecular weight). Recent developments in proteomic technology (*e.g.* Refs. 55–59) should allow some of these difficulties to be overcome and lead to more precise comparative analyses. Also comparison of the same quantity of proteins in either wild-type or mutation-carrying mitochondria, as done here, does not exclude the possibility of larger cellular changes such as regulation in the biogenesis of mitochondria per cell, for example. The two typical mt enzymatic activities measured for both cell lines (citrate synthase and pyruvate dehydrogenase) argue, however, against this possibility. Finally, one should keep in mind that regulation of enzymatic activities does not necessarily involve quantitative variations of their steady-state levels but can be controlled by other biochemical and biophysical means.

Perspectives—The present work used osteosarcoma cybrid cell lines as a model system to explore long range effects of a single mt tRNA gene mutation on the global mt proteome, outside the frame of mt translation. The initial results reported here clearly show the occurrence of such events and open new questions on the molecular mechanisms linking all events. Indeed, it remains to be explored if the observed effects are specifically related to the A8344G mutation or if this is general for other tRNA mutations. Initial studies on cybrid cell lines carrying mutation A3243G in the tRNA$^{Leu(UUR)}$ gene representing a model system of the Mitochondrial Epilepsy, Lactic Acidosis, and Stroke-like episode syndrome already revealed a decrease in two COX subunits, as is the case with the MERRF mutation (21). Furthermore, systematic analysis of cell lines with different nuclear backgrounds for the same tRNA mutation (*e.g.* mutation 8344 in myeloblasts or fibroblasts) should allow one to discriminate between mutation-specific and non-specific perturbations and to decipher the contribution of the nuclear background. The present proteomic investigation, which so far uncovered several unsuspected new players that participate in the disease status of the cell, opens new territory for molecular and biochemical investigation. Their exploration will shed light on the intricate mechanistic pathways linking a

single point mutation in the mt tRNA gene to phenotypic expression of mitochondrial diseases.

Acknowledgments—We are grateful to T. Rabilloud and J. Lunardi for their constructive suggestions on the two-dimensional gel technology and on mitochondrial dysfunction. A. Chomyn and G. Attardi are acknowledged for providing human cybrid cell lines, and G. Lindsay, L. Spremulli, and K. Shiba are acknowledged for the generous gifts of antibodies. We thank C. Prip-Buus for fruitful discussions, M. Sissler for critical comments on the manuscript, L. Levinger for language improvements, and Caroline Paulus for excellent technical assistance.

REFERENCES

1. Scheffler, I. (1999) *Mitochondria*, John Wiley & Sons, Inc., New York
2. Kogelnik, A. M., Lott, M. T., Brown, M. D., Navathe, S. B., and Wallace, D. C. (1998) *Nucleic Acids Res.* **26,** 112–115
3. Ingman, M., Kaessmann, H., Pääbo, S., and Gyllenstein, U. (2000) *Nature* **408,** 708–713
4. Servidei, S. (2001) *Neuromuscul. Disord.* **11,** 508–513
5. Schon, E. A., Bonilla, E., and DiMauro, S. (1997) *J. Bioenerg. Biomembr.* **29,** 131–149
6. Wallace, D. C. (1999) *Science* **283,** 1482–1488
7. Chinnery, P. F., and Turnbull, D. M. (2000) *Mol. Med. Today* **6,** 425–432
8. DiMauro, S., and Andreu, A. (2000) *Brain Pathol.* **10,** 431–441
9. Söll, D., and RajBhandary, U. L. (eds) (1995) *tRNA: Structure, Biosynthesis, and Function.*, American Society for Microbiology, Washington, D. C.
10. Chomyn, A. (1998) *Am. J. Hum. Genet.* **62,** 745–751
11. Chomyn, A., Enriquez, J. A., Micol, V., Fernandez-Silva, P., and Attardi, G. (2000) *J. Biol. Chem.* **275,** 19198–19209
12. Florentz, C. (2002) *Biosci. Rep.* **22,** 81–98
13. Florentz, C., and Sissler, M. (2003) in *Translation Mechanisms* (Lapointe, J., and Brakier-Gingras, L., eds), Landes Biosciences, Georgetown, TX, in press
14. Jacobs, H. T., and Holt, I. J. (2000) *Hum. Mol. Genet.* **9,** 463–465
15. Janssen, G., Maassen, J., and van den Ouweland, J. (1999) *J. Biol. Chem.* **274,** 29744–29748
16. Blackstock, W. P., and Weir, M. P. (1999) *Trends Biotechnol.* **17,** 121–127
17. Celis, J., Kruhoffer, M., Gromova, I., Frederiksen, C., Ostergaard, M., Thykjaer, T., Gromov, P., Yu, J., Palsdottir, H., Magnusson, N., and Orntoft, T. (2000) *FEBS Lett.* **480,** 2–16
18. Jacobs, H. T. (2001) *Trends Genet.* **17,** 653–660
19. Larsson, N., and Rustin, P. (2001) *Trends Mol. Med.* **7,** 578–581
20. Silva, J., and Larsson, N. (2002) *Biochim. Biophys. Acta* **1555,** 106–110
21. Rabilloud, T., Strub, J. M., Carte, N., Luche, S., Van Dorsselaer, A., Lunardi, J., Giegé, R., and Florentz, C. (2002) *Biochemistry* **41,** 144–150
22. Shoffner, J., Lott, M., Lezza, A. M. S., Seibel, P., Ballinger, S. W., and Wallace, D. C. (1990) *Cell* **61,** 931–937
23. Helm, M., Florentz, C., Chomyn, A., and Attardi, G. (1999) *Nucleic Acids Res.* **27,** 756–763
24. Clot, J., Benelli, C., Fouque, F., Rozenn, B., Durand, D., and Postel-Vinay, M. (1992) *J. Clin. Endocrinol. Metab.* **74,** 1258–1262
25. Chomyn, A., Meola, G., Bresolin, N., Lai, S. T., Scarlato, G., and Attardi, G. (1991) *Mol. Cell. Biol.* **11,** 2236–2244
26. Enriquez, J. A., Chomyn, A., and Attardi, G. (1995) *Nat. Genet.* **10,** 47–55
27. Villani, G., and Attardi, G. (1997) *Proc. Natl. Acad. Sci. U. S. A.* **94,** 1166–1171
28. Patel, M., and Korotchkina, L. (2001) *Exp. Mol. Med.* **33,** 191–197
29. Banks, R. E., Dunn, M. J., Hochstrasser, D. F., Sanchez, J. C., Blackstock, W., Pappin, D. J., and Selby, P. J. (2000) *Lancet* **56,** 356–1749
30. Chambers, G., Lawrie, L., Cash, P., and Murray, G. I. (2000) *J. Pathol.* **8,** 192–280
31. Scheffler, N., Miller, S., Carroll, A., Anderson, C., Davis, R., Ghosh, S., and Gibson, B. (2001) *Mitochondrion* **1,** 161–179
32. Mitsumoto, A., Takeuchi, A., Okawa, K., and Nakagawa, Y. (2002) *Free Radic. Biol. Med.* **32,** 22–37
33. Lopez, M. F., and Melov, S. (2002) *Circ. Res.* **90,** 380–389
34. Rabilloud, T., Kieffer, S., Procaccio, V., Louwagie, M., Courchesne, P., Patterson, P., Martinez, P., Garin, J., and Lunardi, J. (1998) *Electrophoresis* **19,** 1006–1014
35. Fountoulakis, M., Berndt, P., Langen, H., and Suter, L. (2002) *Electrophoresis* **23,** 311–328
36. King, M. P., and Attardi, G. (1989) *Science* **246,** 500–503
37. Asoh, S., Mori, T., Hayashi, J.-I., and Ohta, S. (1996) *J. Biol. Chem.* **120,** 600–607
38. Antonicka, H., Floryk, D., Klement, P., Stratilova, L., Hermanska, J., Houstkova, H., Kalous, M., Drahota, Z., Zeman, J., and Houstek, J. (1999) *Biochem. J.* **342,** 537–544
39. Mirabella, M., Di Giovanni, S., Silvestri, G., Tonali, P., and Servidei, S. (2000) *Brain* **123,** 93–104
40. Coenen, M., van den Heuvel, L., and Smeitink, J. A. (2001) *Curr. Opin. Neurol.* **14,** 777–781
41. Garesse, R., and Vallejo, C. (2001) *Gene* (*Amst.*) **263,** 1–16
42. Nijtmans, L., Spelbrink, J. N., Van Galen, M. J. M., Zwaan, M., Klement, P., and Van den Bogert, C. (1995) *Biochim. Biophys. Acta* **1265,** 117–126
43. Nijtmans, L., Taanman, J.-W., Muijsers, A. O., Speijer, D., and Van den Bogert, C. (1998) *Eur. J. Biochem.* **254,** 389–394
44. Bentlage, H. A., Janssen, A. J., Chomyn, A., Attardi, G., Walker, J. E., Schagger, H., Sengers, R. C., and Trijbels, F. J. (1995) *Biochim. Biophys. Acta* **1234,** 63–73
45. Bai, Y., Shakeley, R., and Attardi, G. (2000) *Mol. Cell. Biol.* **20,** 805–815
46. Chomyn, A. (2001) *J. Bioenerg. Biomembr.* **33,** 251–257
47. Tsukihara, T., Aoyama, H., Yamashita, E., Tomisaki, T., Yamaguchi, H., Shinzawa-Itoh, K., Nakashima, R., Yaono, R., and Yoshikawa, S. (1996) *Science* **272,** 1136–1144
48. Cavdar Koc, E., Burkhart, W., Blackburn, K., Moseley, A., Koc, H., and Spremulli, L. L. (2001) *J. Biol. Chem.* **276,** 19363–19374
49. Cavdar Koc, E., Burkhart, W., Blackburn, K., Moyer, M. B., Schlatzer, D. M., Moseley, A., and Spremulli, L. L. (2001) *J. Biol. Chem.* **276,** 43958–43969
50. Kissil, J., Cohen, O., Raveh, T., and Kimchi, A. (1999) *EMBO J.* **18,** 353–362
51. Arden, S., Roep, B., Neophytou, P., Usa, E., Duinkerken, G., and de Vries, R. (1996) *J. Clin. Invest.* **97,** 551–561
52. Wong, P. T., McGeer, P. L., Rossor, M., and McGeer, E. G. (1982) *Brain Res.* **231,** 466–471
53. Kolobova, E., Tuganova, A., Boulatnikov, I., and Popov, K. M. (2001) *Biochem. J.* **358,** 69–77
54. Tan, S., Seow, T., Liang, R., Koh, S., Lee, C., Chung, M., and Hooi, S. (2002) *Int. J. Cancer* **98,** 523–531
55. Gygi, S., Rist, B., Gerber, S., Turecek, F., Gelb, M., and Aebersold, R. (1999) *Nat. Biotechnol.* **17,** 994–999
56. Gygi, S., Rist, B., and Aebersold, R. (2000) *Curr. Opin. Biotechnol.* **11,** 396–401
57. Smolka, M., Zhou, H., and Aebersold, R. (2002) *Mol. Cell. Proteomics* **1,** 19–29
58. Lin, T.-K., Hughes, G., Muratovska, A., Blaikie, F. H., Brookes, P. S., Darley-Usmar, V., Smith, R. A. J., and Murphy, M. P. (2002) *J. Biol. Chem.* **277,** 17048–17056
59. Pflieger, D., Le Caer, J., Lemaire, C., Bernard, B.-A., Dujardin, G., and Rossier, J. (2002) *Anal. Chem.* **74,** 2400–2406